DOI: 10.26599/FSHW.2026.9250912

Contents lists available at SciOpen

Food Science and Human Wellness

journal homepage: https://www.sciopen.com/journal/2097-0765

China Food Publishing Co.

Flammulina velutipes polysaccharide boosts the anti-tumor immunity by reversing M1/M2 polarization through TLR4/NF-κB activation

Chenghao Fu [1†], Ning Chen [1†], Zemiao Niu [1†], Zhenhua Liang [1], Yanwei Huo [1], Rong Chen[2], Yingying Wu[1], Jing Yang[3*], Yan Zhang [4*], Pin Lv [1*]

[1] *Cardiovascular Medical Science Center, Department of Cell Biology, The Key Laboratory of Neural and Vascular Biology, Ministry of Education, The Key Laboratory of Vascular Biomedicine of Hebei Province, Hebei Medical University, Shijiazhuang 050017, China*

[2] *Department of Neurology, Second Hospital of Hebei Medical University, Hebei Key Laboratory of Vascular Homeostasis, Hebei Collaborative Innovation Center for Cardio-cerebrovascular Disease, Shijiazhuang 050000, China*

[3] *Zhejiang Key laboratory of Medical Epigenetics, School of Basic Medical Sciences, Hangzhou Normal University, Hangzhou 310000, China*

[4] *Hebei Food Safety Key Laboratory, Hebei Food Inspection and Research Institute, Shijiazhuang 050091, China*

ABSTRACT: Macrophage polarization is a pivotal determinant in the modulation of immune responses and the formation of the tumor-microenvironment (TME), therefore represents a promising avenue for the development of cancer immunotherapy. Recent research highlights the potential of edible mushroom polysaccharides in inducing M1/M2 polarization of macrophages. Here, we report that oral administration of *Flammulina (F.) velutipes* polysaccharide (FVP) reduced the tumor volume of grafted 4T1 mammary and lewis lung carcinoma (LLC), and increased the overall survival rate of mice. Moreover, this polysaccharide induced the generation of $CD11b^{+}Ly6C^{high}F4/80^{+}$ macrophage cells in LLC and 4T1 tumor-bearing mice. Further investigation found that FVP decreased the ratio of M2-macrophages and regulatory T cells in TME, which is known to support tumor growth and metastasis. Mechanistically, FVP reversed the IL-4 induced M2-polarization by activating the TLR4/ NF-κB axis, and in vitro assays confirmed the expression of pro-inflammatory genes and the antitumor effects of the polysaccharide. Additionally, the expression of Th1 response relative genes also enhanced by FVP polarized macrophage secretions. In summary, these results suggest that FVP may represent a promising immunomodulatory agent for the reversal of macrophage polarization.

Keywords: *F. velutipes* polysaccharide, Lewis lung carcinoma, 4T1 mammary carcinoma, anti-tumor immunity, macrophages, M1/M2 polarization

1. Introduction

Cancer immunotherapy offers several advantages over chemotherapy, including its ability to specifically target cancer cells, provide long-term protection against cancer recurrence, and offer personalized treatment plans [1, 2]. These advantages make it a promising approach to cancer treatment that has the potential to improve patient outcomes and quality of life [1, 3]. However, several barriers still exist that limit its efficacy and

† These authors have contributed equally to this work
***Corresponding author**
Pin Lv, lvpin@hebmu.edu.cn; Yan Zhang, snowwinglv@126.com
Jing Yang, 20220059y@hznu.edu.cn

Received 22 September 2025
Received in revised from 3 November 2025
Accepted 2 December 2025

applicability, with one of the primary challenges being the tumor microenvironment (TME), which can be immunosuppressive and prevent the activation and infiltration of immune cells [4]. The immunosuppressive system in the TME consists of regulatory T cells (Tregs), myeloid-derived suppressive cells, regulatory dendritic cells, and M2 macrophages [5-7]. M1 and M2 macrophages are two functionally distinct subsets of macrophages with different roles in the TME. M1 macrophages are pro-inflammatory and promote immune responses to pathogens or tumors, while M2 macrophages are anti-inflammatory and characterized by the expression of specific markers such as CD206, CD163, and arginase1 (ARG1), as well as the production of anti-inflammatory cytokines such as interleukin 10 (IL-10) and transforming growth factor-beta (TGFβ) [5-7]. M2 macrophages are induced by the presence of Th2 cytokines, such as IL-4, IL-13, and IL-10, or by the presence of immune complexes and apoptotic cells. Evidence suggests that M2 macrophages can be reprogrammed toward an M1 phenotype by exposing them to pro-inflammatory cytokines, such as interferon-gamma (IFN-γ) and lipopolysaccharide (LPS), which is one of the approaches utilized to enhance anti-tumor immunity [8].

Edible mushroom polysaccharides have shown significant potential as immunomodulatory agents [9-12]. Compared to chemical agents, polysaccharides have several advantages in stimulating the immune system, such as being generally safe and well-tolerated, having potent activity to enhance immune response, and being easily obtained from a variety of sources [9, 10]. These advantages make mushroom-derived polysaccharides promising candidates for the development of novel immunomodulatory agents for the treatment of cancer. In recent years, polysaccharide extracts from edible mushrooms have been widely used in pre-clinical or clinical practice [11, 13, 14]. For example, Xu and colleagues found a new *Lentinula edodes*-derived 26 kDa heteropolysaccharide that activates RAW264.7 cells via the TLR4 signaling pathway [15], while Chen and his team isolated β-D-(1→6) glucan from Amillariella Mellea, which could promote the transformation of M2 macrophages to the M1 phenotype and inhibit the viability of colon cancer cells in vitro and in vivo [16]. Collectively, the above facts suggest that immune cell reprogramming, especially macrophages, plays an essential role in the anti-tumor effects triggered by polysaccharide.

Flammulina velutipes (F. velutipes), also known as the golden needle mushroom, is a large edible and medicinal fungus with abundant nutritional and medicinal value. Further research in recent years has shown that polysaccharides are one of the main active components of *F. velutipes*, possessing various bioactivities such as antioxidative, immunomodulatory, anti-inflammatory, liver protection, anti-tumor, and anti-hyperlipidemia effects [17]. In fact, since 1995, *F. velutipes* polysaccharides (FVP) have been found to be effective against solid tumors, and their anti-tumor activity has been shown to be mediated by the tumor-bearing host [18]. Further studies have also demonstrated that subfractions of FVP exhibits anti-proliferation activity against human gastric cancer BGC-823 cells, lung cancer A549 cells, and murine melanoma B16F10 cells in vitro [19, 20]. Recently, several reports have shown that FVP exhibits excellent immuno-stimulating activity, including increased phagocytic activity of RAW264.7 cells and the reversal of cyclophosphamide-induced immunosuppression effects in vivo [10, 21]. In summary, the available evidence

suggests that FVP has potential anti-tumor effects, but further research is needed to fully understand the mechanisms involved and to explore their potential therapeutic applications.

In this study, we reported that FVP inhibits the progression of Lewis Lung Carcinoma (LLC) and 4T1 mammary carcinoma and skews M1/M2 macrophage polarization induced by IL-4, both in vitro and in vivo. The possible molecular mechanisms responsible for the converting effects were further discussed.

2. Materials and methods

2.1 Animals

BALB/c (female) and C57BL/6 (male) mice, aged 8-10 weeks, had free access to food and water and were kept under constant conditions of temperature (23℃ ± 1℃) and humidity (60%) prior to experiments. The animals were housed under specific pathogen-free conditions with 12 h day/light cycles. All animal studies were conducted according to protocols approved by the Animal Ethics Committee of the Hebei Food Inspection and Research Institute (Approval No.: IACUC-SC-2020-2).

2.2 Cell Lines and Tumor Cell Injection

Lewis lung carcinoma (LLC), 4T1 tumor cells, and RAW264.7 cells were purchased from the Cell Bank of the Chinese Academy of Sciences (Shanghai, China). LLC and 4T1 cells were cultured in high-glucose Dulbecco's modified Eagle's medium (DMEM) or RPMI-1640 medium respectively. Both medium supplemented with 10% (v/v) fetal bovine serum (FBS), 2 mmol/L glutamine, 100 U mL^{-1} penicillin, and 100 μg/mL streptomycin (Gibco, Grand Island, NY, USA) at 37℃ with 5% CO_2.

LLC or 4T1 cells were used to establish a subcutaneous cancer mouse model. Prior to injection, cells in the log phase of growth were harvested and suspended in phosphate-buffered saline (PBS) from Solarbio (Beijing, China). The tumor volume was calculated using the following formula [22]: tumor volume (mm^3) = (length × width × width)/2.

2.3 In vivo F. velutipes polysaccharide treatment

FVP was obtained according to the protocol detailed in reference [10, 23]. The dried powder of F. velutipes was successively extracted by petroleum ether and 75% ethanol (1:2, w/v; 2 times for 72 h each) to remove the fat-soluble components, then extracted by hot water (1:30, g/mL) three times at 80℃ for 4 h each, and the filtrate was precipitated with 70% ethanol at 4 ℃ for 24 h. The precipitates were washed with anhydrous ethanol, acetone and petroleum ether three times, and then freeze-dried to obtain crude polysaccharide. The dried polysaccharides were resuspended in water, treated with Sevag reagent (chloroform:n-butanol = 4:1, v/v), and centrifuged (7000 r/min, 10 min) to remove the proteins, this procedure was repeated 10 times. After precipitation with 70% ethanol, FVP was freeze-dried and stored at room temperature.

To determine the anti-tumor efficacy of FVP on LLC and 4T1 allograft tumors, the tumor-bearing mice (n=5 per group) received 100 mg/kg of FVP via oral gavage for 14 consecutive days. Mice in control groups received the same volume of distilled water daily by gavage. The tumor-bearing mice were maintained until their tumors reached 2 cm in any dimension at 14 days after FVP treatment. The peripheral blood, spleen,

lung, bone marrow, and tumor mass were collected for flow cytometry (FCM) and immunohistochemistry (IHC) detection.

2.4 Ex vivo Splenic Cells and Macrophages Culturation

Euthanize the mice under sterile conditions and collect the spleen. The spleen was gently homogenized in RPMI 1640 and passed through a 70 μm nylon mesh. RBCs were removed using ACK lysis buffer. Splenic single cells were plated at a density of 1-2 × 10^6 cells/well in 6-well plates and suspended in glucose-free DMEM from Gibco or RPMI 1640 medium. After incubation at 37℃ under 5% CO_2 for 12 h, the cells were washed twice with PBS and analyzed by FCM.

Three days before the experiment, 2 mL of sterile 4% thioglycolate medium (BD Biosciences, San Jose, CA, USA) was injected into the peritoneal cavity of each mouse. Euthanize the mcie under sterile conditions and collect the ascites. Suspensions of 1-2 × 10^6 cells in 6-well plates were prepared in RPMI 1640 medium. The medium was replaced 6-8 h later to harvest the macrophages. To examine cell surface markers, peritoneal macrophages (PMs) were cultured in medium supplemented with 20 ng/mL IL-4 or 50 μg/mL FVP for 24 h.

To evaluate the cytotoxic effects of cytokines from FVP-induced polarized macrophages on tumor cells, RAW264.7 cells were treated with 50 μg/mL FVP for 24 hours, followed by three PBS washes and 12 hours of culture in fresh medium to collect the conditioned medium (RAW-CM). LLC cells were cultured to 70%–80% confluency, washed three times with PBS, and cultured for 12 hours in fresh medium to obtain the LLC tumor cell-conditioned medium (LLC-CM).

2.5 Flow Cytometry and Antibodies

The preparation of single-cell suspension was described previously [24]. Antibodies specific for the following surface markers were used: CD45 (30-F11), CD11b (M1/70), CD3e (145-2C11), CD4 (Gk1.5), CD8a (53-6.7), CD25(PC61), CD80(1610A1), CD16/32(93), MHCII (M5/114.15.2), CX3CR1 (SA011F11), CD163 (S15049I), CD206 (MR6F3), Sca-1 (D7), C-kit (ACK2), CD34 (SA376A4), Ly6C (HK1.4), Ly6G (1A8-Ly6g), and F4/80 (BM8) were purchased from Biolegend (San Diego, CA, USA) or eBioscience (San Diego, CA, USA); antibodies were used at the dilutions recommended by the manufacturer. Laser voltages were set using unstained cells, single stain, fluorescence minus one control, and isotype controls for compensation. Flow cytometry was performed with CytoFLEX SRT (Beckman Coulter, USA) and BD FACS Verse (BD Biosciences, USA), and data were analyzed with FlowJo v. 10 (BD Biosciences, USA).

Before gating $CD45^+$ cells, five steps were performed: (1) Flow stability gating (Time vs Side Scatter) to ensure stable flow; (2) Scatter gating (Forward vs Side Scatter) to remove debris and off-scale events; (3) Doublet gating (Forward Scatter height vs area) to remove doublets; (4) Viability gating to remove dead cells; and (5) $CD45^+$ cell gating to identify the $CD45^+$ subset[24, 25]. All flow cytometry data shown in this manuscript are based on this strategy.

For the evaluation of phagocytic capacity, RAW264.7 cells were pre-treated with 20 ng/mL IL-4 or 50 μg/mL FVP for 24 h, followed by addition of 50 μg/mL dextran-FITC for 30 min of culture.

2.6 Apoptosis Assay

Apoptotic cells were detected with a FITC Annexin V apoptosis detection kit (BioLegend, USA) followed by surface marker staining and flow cytometry analysis. Early apoptotic cells were defined as Annexin V-positive and PI negative. Late apoptotic cells were designated Annexin V-positive and PI positive.

2.7 Immunohistochemistry (IHC)

Tissues from mice were fixed in 4% paraformaldehyde, processed, embedded in paraffin, and sectioned.[26]. Paraffin was removed with two 10-minute xylene treatments, and sections were then hydrated through an alcohol series and soaked in distilled water for 2 min. Antigen retrieval was performed using microwaving and sodium citrate (pH 6.0). After blocking with 5% bovine serum albumin for 1 hour at 37℃, sections were incubated with anti-Ki67, cleaved caspase 3, CD206, and iNOS antibodies at 4℃ overnight. The sections were incubated with a biotinylated secondary antibody and streptavidin-conjugated horseradish peroxidase, followed by diaminobenzidine (DAB) (ZSGB-BIO, China) and counterstained with Gill's hematoxylin (Fisher Scientific, USA). Subsequently, sections were sealed with the sealing solution and imaged under a microscope (Leica Microsystems, Germany).

2.8 Quantitative real-time PCR

Total RNA was extracted using TRIzol reagent (Invitrogen), and cDNAs were synthesized using reverse transcriptase SuperScript II (Invitrogen). Quantitative real-time PCR (qRT-PCR) was performed using SYBR Green RT-PCR Master Mix (Invitrogen) and the 7300 Real Time PCR System (Applied Biosystems, Carlsbad, CA, USA). Mouse IL-1β, IL-6, iNOS, MCP1, TNF-α, IL-12a, IL-12b, TGFβ, IL-10, ARG1, CD163, H2EB1, CD86, TOP1, mTOR, Ki67, CDK2, IL-2, PD-1, Granzyme B (GZB), IFNγ were normalized to that of GAPDH and reported as relative mRNA expression ($\Delta Ct=2^{-\Delta Ct\ sample\ -\ \Delta Ct\ control)}$). The specific primers used for qRT-PCR analysis were provided in Supplemental Table 1.

2.9 Immunofluorescence assay

To perform immunofluorescent staining, RAW264.7 or PMs on coverslips were fixed in 4% paraformaldehyde for 30 min, permeabilized with PBS containing 0.1% Triton X-100, blocked with 5% normal goat serum in PBS, incubated with an p65 antibody (ABclonal, China) overnight at 4℃, washed with PBS, and incubated with a fluorescein-conjugated secondary antibody (KPL, USA) for 1 h at room temperature. Cells were then stained with DAPI (Sigma, Germany) for 5 min, and images were obtained using a Confocal Laser Scanning Microscope System (Leica Microsystems, Germany).

2.10 Western blot analysis

Protein was extracted from RAW264.7 cells and protein concentrations were determined using the BCA assay (Beyotime, China). Equal protein amounts were separated on SDS-PAGE gels and transferred to PVDF membranes (Millipore, USA). The membranes were blocked with 5% nonfat dried milk, probed with primary antibodies (anti-TLR4, anti-Ikkα/β, anti-p-p65, or anti-β-actin; ABclonal, China) at 4℃ overnight, and

incubated with horseradish peroxidase-conjugated secondary antibody at room temperature for 1 h. The blots were visualized using an ECL kit (Beyotime, China). The protein bands of interest were quantified using Image Pro Plus 6.0 software.

2.11 Statistical analysis

All experiments were repeated at least three times, and data collection and analysis were performed in a blinded manner with respect to the experimental group. Only representative data are presented. Statistical analysis was conducted using GraphPad Prism v. 6 (GraphPad Software, USA) and Microsoft Excel 2016 (Microsoft Corporation, USA).

Normally distributed data were analyzed using unpaired or paired Student's t-tests for two-group comparisons, and one-way ANOVA followed by Bonferroni's post hoc test for multiple groups. Unless otherwise indicated, significance was determined as follows: ***$P < 0.001$, **$P < 0.01$, and *$P < 0.05$.

3.1 Results

3.1 F. velutipes polysaccharide delayed the progression of LLC and 4T1 cancer in mice

To evaluate the anti-tumor efficiency of FVP, 1×10^6 LLC and 4T1 tumor cells were injected subcutaneously into C57/BL6 and BALB/c mice, respectively. Mice with similar tumor volumes were used to maintain initial tumor-size homogeneity (Figure 1A). After 14 consecutive days of gavage, we observed the grafted tumor volume in LLC-FVP and 4T1-FVP groups was reduced by 30% and 40%, respectively, compared to that of the control groups (Figure 1B and 1C). In addition, the overall survival data show that over 20% of the mice in LLC-FVP and 4T1-FVP groups survived on day 60 after tumor grafting (Figure 1D and 1E). Furthermore, we also examined the Ki67 expression in lung and tumor tissues using IHC assays, and the results show that the Ki67 expression in LLC-FVP and 4T1-FVP groups decreased to 80% and 70% of that in the control groups (Figure 1F-1H). Additionally, the Cleaved caspase 3 in tumor of LLC-FVP groups also showed an upward trend, which was consistent with the decreasing trend of that in 4T1-FVP groups (Figure 1I). The above results suggest that oral absorption of FVP delays the tumor progression via inhibiting the proliferation rate of cancer cells.

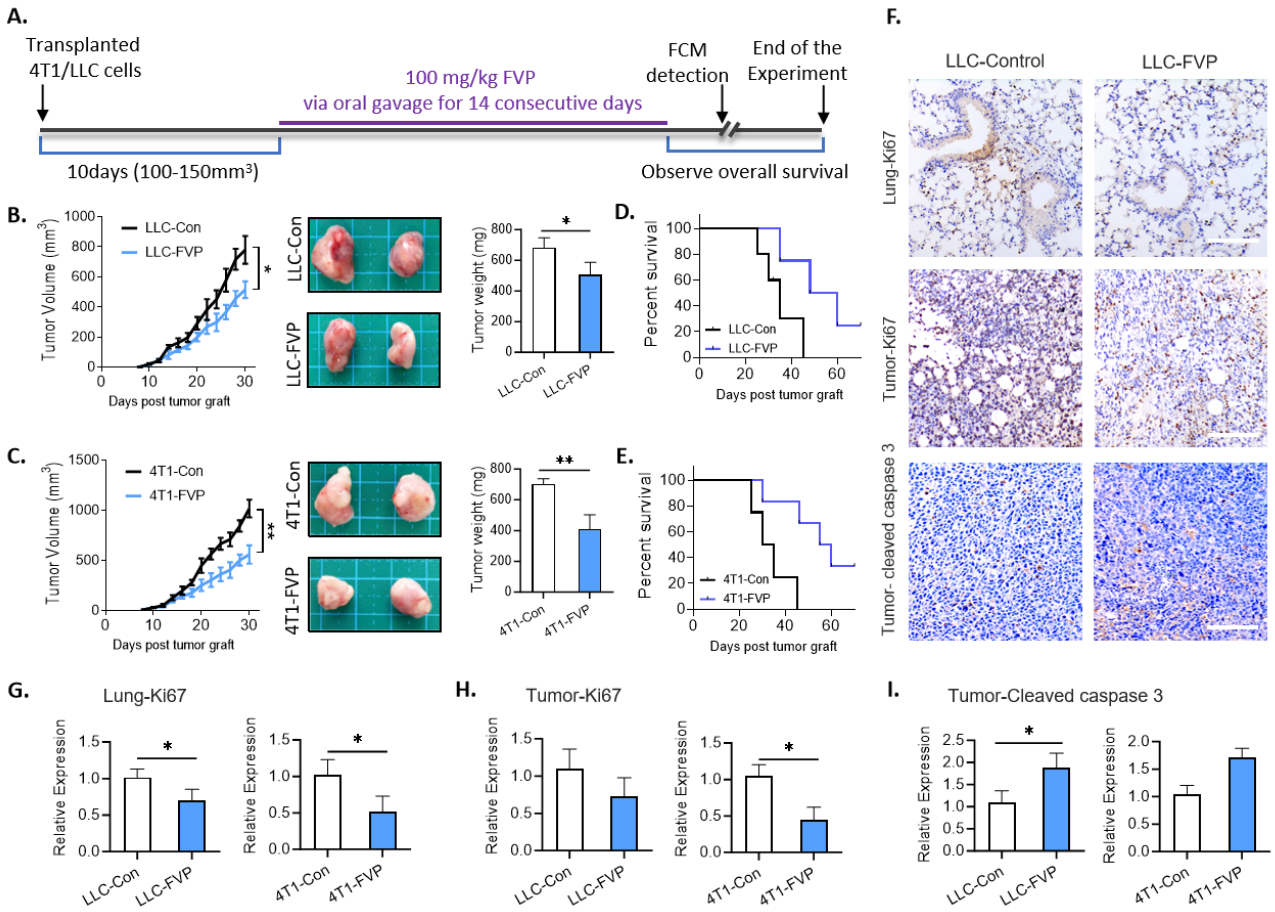

Figure 1 *F. velutipes* polysaccharide delayed the progression of LLC and 4T1 cancer in mice
Mice in both LLC and 4T1 groups were implanted with 1×10^6 tumor cells. Ten days post-transplantation, LLC-Con and 4T1-Con mice were gavaged with water, while LLC-FVP and 4T1-FVP mice were gavaged daily with 100 mg/kg FVP for 14 days. (A) after the completion of FVP treatment, the tumor-bearing mice were either sacrificed for tissue collection or euthanized when their tumors reached 2 cm in any dimension. (B-E) Tumor volume, tumor weight, and overall survival curve in LLC group (B, D) and 4T1 groups (C, E). (F) Representative images of Ki67 and cleaved caspase 3 immunohistochemical (IHC) staining in lung and tumor tissues, bar=100μm. (G-I) The relative Ki67 and cleaved caspase 3 expression in indicated groups. Data represent ≥ 3 independent experiments and are shown as means ± standard deviation. *$P < 0.05$, **$P < 0.01$, ***$P < 0.001$.

3.2 F. velutipes polysaccharide increased the CD11b$^+$F4/80$^+$ cells in LLC and 4T1 tumor-bearing mice

FVP has been shown to be effective against solid tumors, with its anti-tumor activity mediated by the immune system of the tumor-bearing host [18]. Myeloid subsets, such as macrophages, monocytes, and neutrophils, play a critical role in mediating this anti-tumor effect. Therefore, we collected peripheral blood, spleen, and lung samples from healthy and tumor-bearing mice to investigate the changes in myeloid immune cells using flow cytometry. Necessary steps, such as removing unstable flow, debris, off-scale events, doublets, dead cells, and non-CD45$^+$ cells, were taken prior to analyzing the myeloid subpopulations of FCM data [24, 27].

The results showed that the ratio of CD11b$^+$Ly6C^{high}Ly6G$^-$ monocytes in the 4T1-Con and LLC-Con groups increased significantly or showed a tendency to increase compared to that in the healthy group, and the increasing trends were reversed when treated with FVP, except for that in the blood of LLC tumor models (Figure 2A-2H). The ratio of CD11b$^+$Ly6C^{high}Ly6G$^-$ granulocytes substantially increased on day 24 after

tumor grafts, and treatment with FVP did not cause a consistent alteration (Figure 1A and 2A-2H). Regarding the CD11b^{+}F4/80^{+} macrophage cells, there was a significant decrease in the 4T1-Con and LLC-Con groups compared to the healthy group, but treatment with FVP induced an increasing trend in the collected tissues (Figure 2A-2H). Overall, these results indicate that FVP had a deep impact on the circulation myeloid subpopulation and increased the CD11b^{+}F4/80^{+} cells in LLC and 4T1 tumor-bearing mice.

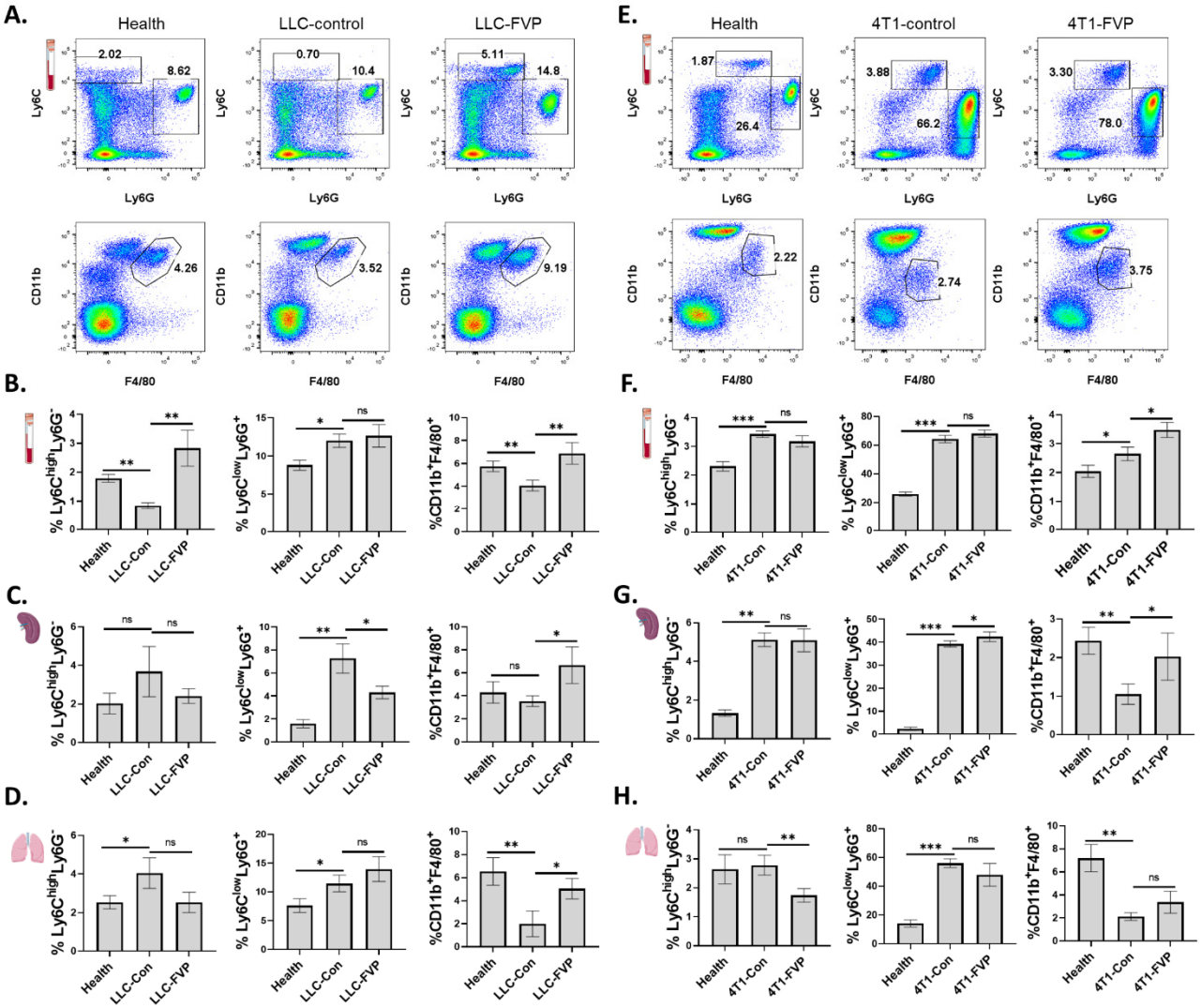

Figure 2 *F. velutipes* polysaccharide increased the CD11b^{+}F4/80^{+} cells in LLC and 4T1 tumor-bearing mice
LLC and 4T1 tumor-bearing were euthanized on day 14 after FVP treatment, and the peripheral blood, spleen, and lung were collected for flow cytometry (FCM) detection. (A) Representative FCM plots data of the peripheral blood immune cells in LLC tumor-bearing mcie. (B-D) Frequency of CD11b^{+}Ly6C^{high}Ly6G^{-}, CD11b^{+}Ly6C^{low}Ly6G^{+}, and CD11b^{+}F4/80^{+} cells in the blood (B), spleen (C) and lung (D). (E) Representative FCM plots of peripheral blood immune cells in 4T1 tumor-bearing mcie. (F-H) Frequency of CD11b^{+}Ly6C^{high}Ly6G^{-}, CD11b^{+}Ly6C^{low}Ly6G^{+}, and CD11b^{+}F4/80^{+} cells in the blood (F), spleen (G) and lung (H). Data represent ≥ 3 independent experiments and are shown as means ± standard deviation. *P < 0.05, **P < 0.01, ***P < 0.001.

3.3 F. velutipes polysaccharide promoted the GMP generation in bone marrow

Macrophages differentiate from monocytes, which are formed in hematopoietic precursor cells in the bone marrow [28]. Herein, we collected the bone marrow cells on day 24 after tumor grafts, and C-kit^{+}Sca-1^{+} cells were pre-gated on non-dead and CD45 positive cells (Figure 3A). The gating strategy of LK (C-kit^{-}Sca-1^{+}), LSK (C-kit^{+}Sca-1^{+}), granulocyte macrophage progenitor (GMP, C-kit^{-}Sca-1^{+} CD16/32^{high}

CD34^{+}), common myeloid progenitor (CMP,), and megakaryocyte erythroid progenitor (MEP, C-kit^{-}Sca-1^{+} CD16/32^{-} CD34^{-}) cells was based on published literature[28, 29]. We observed that, compared to health-groups, the ratio of LSK, LK, and CMP increased significantly in LLC-Con groups, and FVP gavage enhanced this alteration (Figure 3B and 3C). The GMP and MEP in bone marrow reduced by 40% of that in health control groups, and FVP helps recovered to normal (health control group) levels. And splenic GMPs alteration exhibited a similar trend to that in bone marrow. Overall, these results imply that FVP alters the GMP generation in bone marrow.

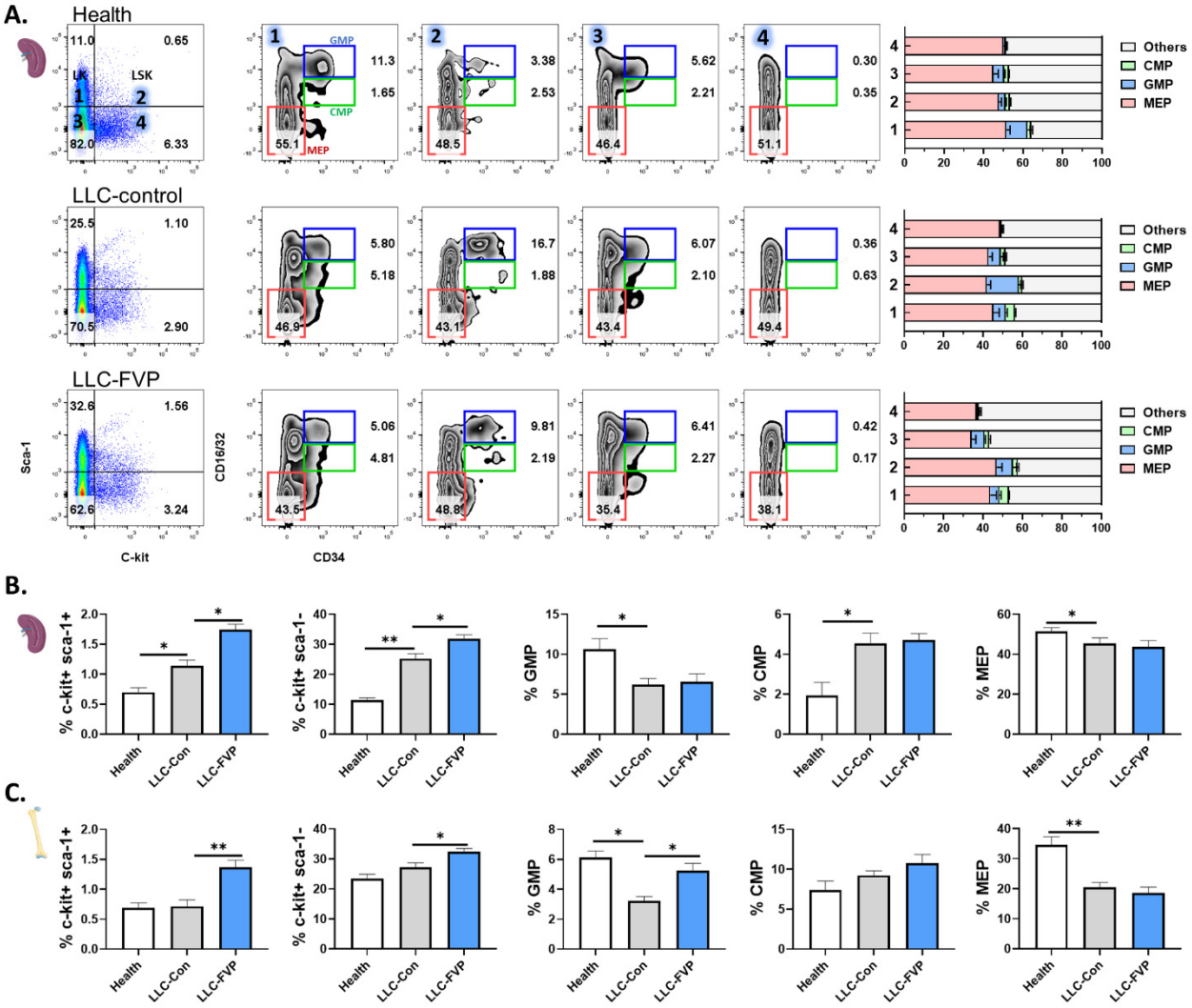

Figure 3 *F. velutipes* polysaccharide promoted the GMP generation in bone marrow.
The spleen and bone marrow of LLC tumor-bearing mcie were collected for FCM detection on day 14 after FVP treatment. The C-kit and Sca-1 gates were pre-gated on CD45^{+}Lin^{-} cells. (A) Representative FCM plots of splenic myeloid progenitor cells subsets. GMP, granulocyte-macrophage progenitor; CMP, common myeloid progenitor; MEP, megakaryocyte-erythroid progenitor. (B-C) The percentage of LK (Lin^{-}Sca-1^{+}c-Kit^{-}), LSK (Lin^{-}Sca-1^{+}c-Kit^{+}), GMP, CMP, and MEP cells in the spleen(B) and bone marrow (C). Data represent ≥ 3 independent experiments and are shown as means ± standard deviation. *P < 0.05, **P < 0.01, ***P < 0.001.

3.4 F. velutipes polysaccharide reduced the ratio of M2 macrophages and Tregs in TME

We next examined the relative expression of anti-iNOS and CD206 on tumor tissues via IHC assays (Figure 4A). The data show that iNOS in LLC-FVP groups has grown by at least 2-fold, and an increment trend was also observed in 4T1-FVP groups. In addition, CD206 showed decreased trends in both LLC and

4T1-FVP groups (Figure 4B). Moreover, we detected the expression of CD80, CD16/32, MHC II, CX3CR1, CD163, and CD206 in $CD11b^{+}F4/80^{+}$ macrophages of tumor microenvironments (TME) from LLC-Con and LLC-FVP groups (Figure 4C). The results show that the relative expression of CD80, CD16/32, MHC II, CX3CR1, and CD163 was increased, and CD206 significantly decreased in LLC-FVP groups compared to that in LLC-Con groups (Figure 4D). The above data suggests FVP promotes the percentage of M1 macrophages in the TME. Research has shown that macrophages and Tregs can interact in the TME. M2 macrophages can promote the recruitment and expansion of Tregs, while Tregs can in turn inhibit the activation and polarization of M1 macrophages [8, 30]. Therefore, we examined the alteration of Tregs in the TME, and the data show $CD3^{+}CD4^{+}CD25^{+}$ Treg cells reduced to half of that in TME after FVP treatment (Figure 4E). Collectively, the above data suggest that FVP have the ability to alter M1/M2 polarization in the cancer model.

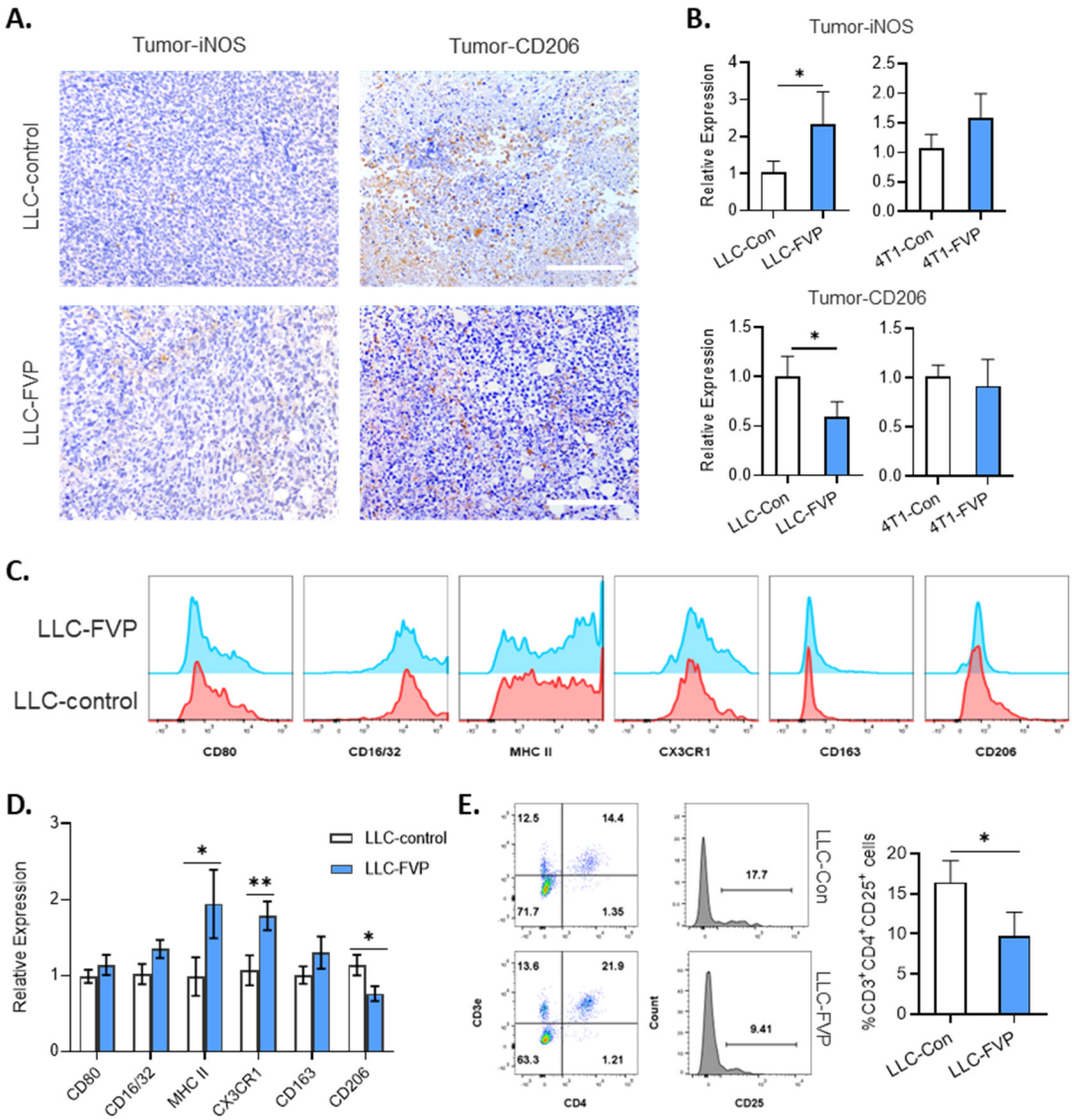

Figure 4 *F. velutipes* polysaccharide reduced the ratio of M2 macrophages and Tregs in TME
The tumor mass of LLC tumor-bearing mcie were collected on day 14 after FVP treatment. (A) Representative images of iNOS and CD206 IHC staining in tumor, bar=100μm. (B) The relative expression level of iNOS and CD206 in LLC and 4T1 tumor tissue. (C-E) LLC tumor tissuce was collected and digested into single cells for FCM analysis. (C-D) The histogram FCM data of $CD11b^{+}F4/80^{+}$ cells surface markers. (E) The ratio of $CD3^{+}CD4^{+}CD25^{+}$ T cells in TME. Data represent ≥ 3 independent experiments and are shown as means ± standard deviation. *$P < 0.05$, **$P < 0.01$, ***$P < 0.001$.

3.5 F. velutipes polysaccharide reversed IL4 induced M1/M2 polarization

M1 and M2 macrophages are two functionally distinct subsets of macrophages with different roles in the immune response. M1 macrophages are pro-inflammatory and are involved in promoting immune responses to pathogens or tumors, while M2 macrophages are anti-inflammatory and are involved in tissue repair and resolution of inflammation[8, 30]. The polarization of macrophages towards the M2 phenotype can be induced by IL-4, which activates STAT3, STAT6, or IFR4 signaling pathways to induce the expression of IL-10, ARG1, TGFβ[31]. We observed that treatment with 50μg/mL FVP improved the relative mean fluorescence intensity of CD86, CD16/32, MHC II, and CD163 molecules in IL-4 pre-treated RAW264.7 and peritoneal macrophages (Figure 5A-5C). Another hallmark function of M1 macrophages is their high phagocytic capacity[32]. Dextran-FITC was utilized to examine the phagocytosis rate of macrophages. When RAW264.7 was treated with 20 ng/mL IL-4, the phagocytic capacity was significantly decreased, and FVP can reverse the trend in a dose dependent manner (Figure 5D). In addition, LLC-CM also increased the phagocytic capacity of RAW264.7, and FVP displayed a synergistic effect to increase the phagocytosis rate (Figure 5E). In general, these findings imply that FVP promotes the switch of macrophages to the M1 phenotype.

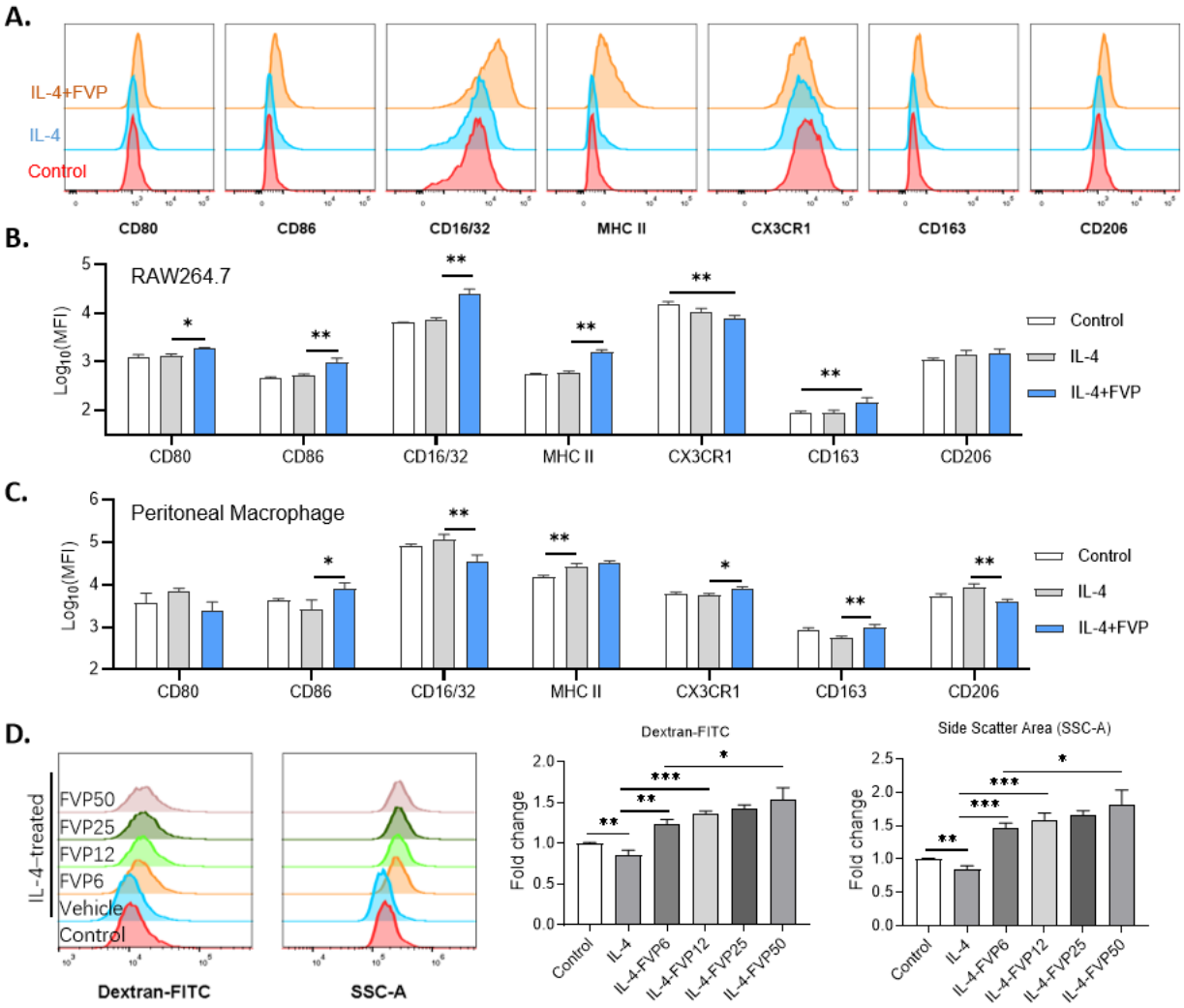

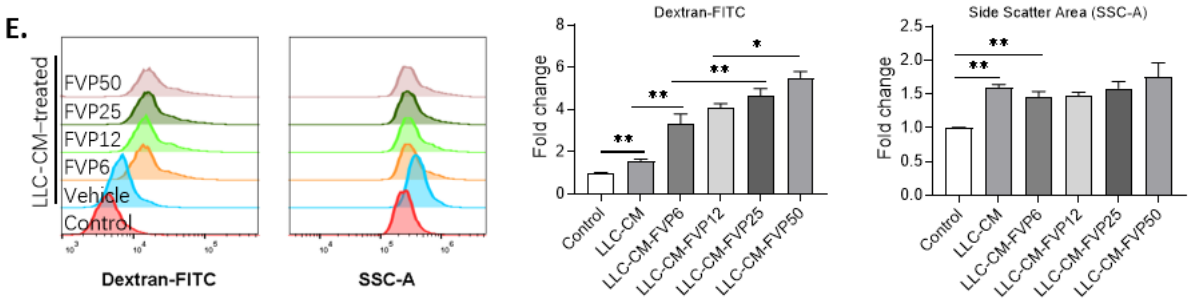

Figure 5 *F. velutipes* polysaccharide reversed IL4-induced M1/M2 polarization.
The RAW264.7 and peritoneal macrophages (PMs) were pre-cultured with IL-4 for 8 hours, and then, after the addition of FVP (or PBS) to the medium, the culture was continued for an additional 24 hours. (A) Representative histogram FCM data of RAW264.7. (B) The mean fluorescence intensity (MFI) of cell surface marker on RAW264.7. (C) The MFI of cell surface marker on PMs. The ability of phagocytic capacity was measured by the cellular uptake of Dextran-FITC. (D) The phagocytic capacity alteration of RAW264.7 after IL-4 and FVP treatment. (E) Alteration of phagocytic capacity in RAW264.7 cells after LLC tumor-conditioned medium (LLC-CM) and FVP treatment. Data represent ≥ 3 independent experiments and are shown as means ± standard deviation. *$P < 0.05$, **$P < 0.01$, ***$P < 0.001$.

3.6 F. velutipes polysaccharide increased the antitumor effects via activating M1 macrophages

We examined the gene expression of inflammation-related genes in RAW264.7 cells treated with IL-4 or FVP. The results showed that IL-4 treatment inhibited the expression of iNOS, TNF-α, IL-12a, TGFβ, CD163, H2eb1, and CD86, while the addition of FVP substantially increased their expression (Figure 6A). Additionally, consistent with the findings in Figure 5E, FVP showed a synergistic effect in increasing the expression of IL-1β, MCP1, and IL-12b when pretreated with IL-4 or LLC-CM (Figure 6B).

To evaluate tumor cell migration and apoptotic rate, we used scratch assays and Annexin V/PI assays, respectively. The control groups were treated with RAW-CM without FVP. We found that both the migration and pro-apoptotic capacity were promoted in a dose-dependent manner (Figure 6C and 6D). Moreover, we observed a significant reduction in the gene expression of TOP1, mTOR, Ki67, and CDK2 under the treatment of RAW-CM, suggesting that cytokines released by M1 macrophages mediated the inhibition of LLC (Figure 6E).

To determine whether M1-released cytokines promote the anti-tumor effects in lymphocytes, splenic lymphocytes were separated via Percoll gradient medium and treated with RAW264.7 condition medium. The results showed that TNF-α, GZB, and IFNγ increased at least 4-fold, and PD-1 decreased 3-fold compared to the control groups (Figure 6F). Collectively, these results indicate that FVP boosts the antitumor effects via activating M1 macrophages.

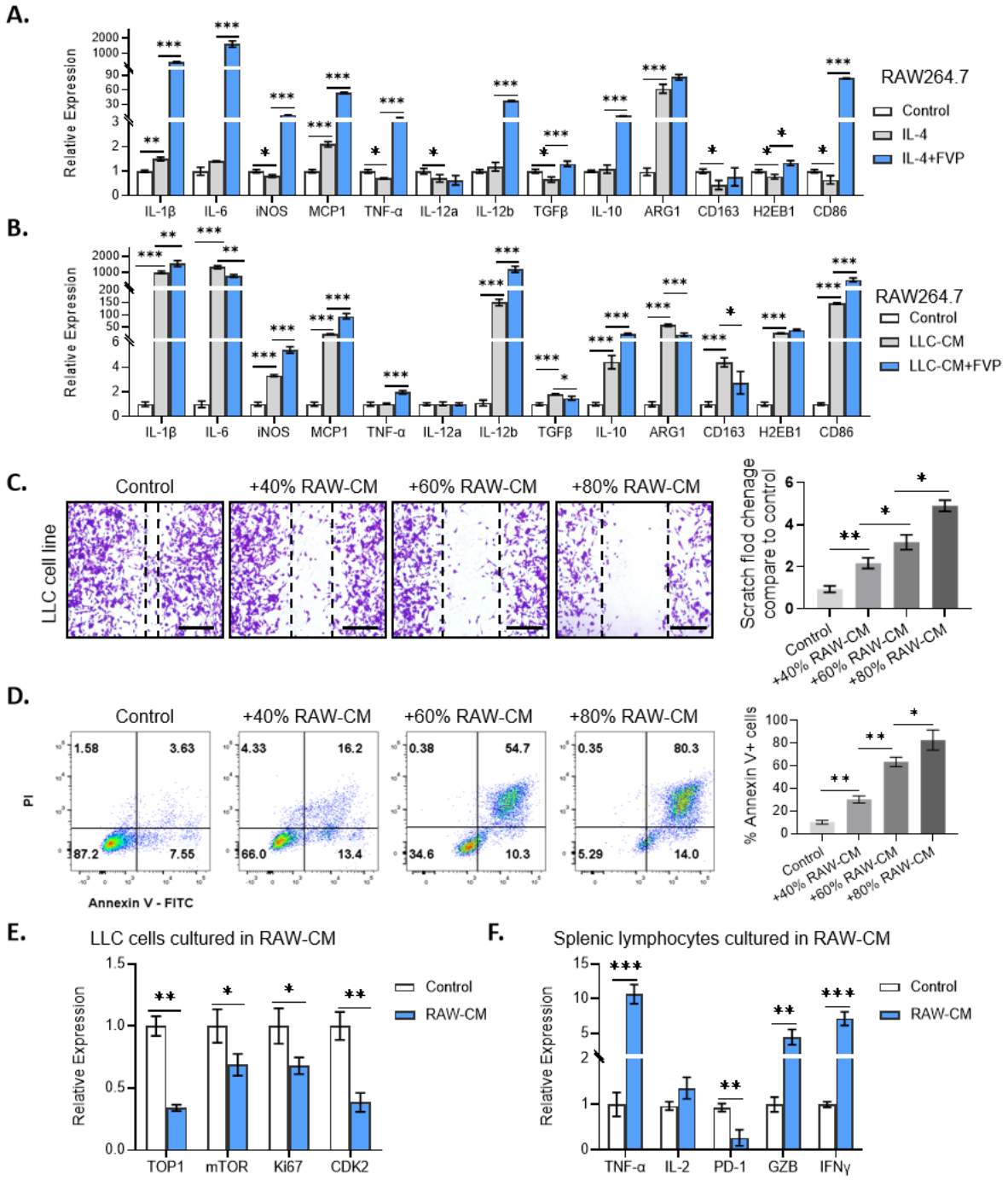

Figure 6 *F. velutipes* polysaccharide increase the antitumor effects via activating M1 macrophages (A)The relative gene expression of RAW264.7 cells after IL-4 or FVP treatment. (B) The relative gene expression of RAW264.7 cells after LLC-CM or FVP treatment. The RAW-CM was obtained from the conditioned medium of RAW264.7 under FVP treatment. The LLC cells were harvested for the scratch and apoptosis assays after co-cultured with FVP treated RAW-CM for 24 hours. 40%, 60%, 80% RAW-CM means 40%, 60%, 80% of the medium was repalced by RAW-CM. The LLC cells in control groups were treated with RAW-CM without FVP. (C) Relative scratch wound closure in LLC cells. (D) The apoptotic rate of LLC tumor cells. (E) The relative gene expression of LLC cells after RAW-CM treatment. (F) The relative gene expression of splenic lymphocytes after RAW-CM treatment. Data represent ≥ 3 independent experiments and are shown as means ± standard deviation. *$P < 0.05$, **$P < 0.01$, ***$P < 0.001$.

3.7 F. velutipes polysaccharide induced the activation of TLR4/NF-κB axis

Activation of macrophages by polysaccharides typically involves a series of signaling events and transcriptional regulation [9, 33]. Polysaccharide-induced activation of toll-like receptors (TLRs), mannose receptors, and other pattern recognition receptors (PRRs) triggers a signaling cascade that leads to the

activation of the inhibitor of κB kinase (IKK) complex. The activated IKK complex then phosphorylates the inhibitor of κBα (IκBα), leading to its ubiquitination and subsequent degradation by the proteasome [9, 34]. Based on this background knowledge, we examined the key proteins of the TLR4/NF-κB signaling pathway via western blot assays. The results showed that the relative expression of TLR4 and p-p65 significantly increased in FVP-treated RAW264.7 cells (Figure 7A).

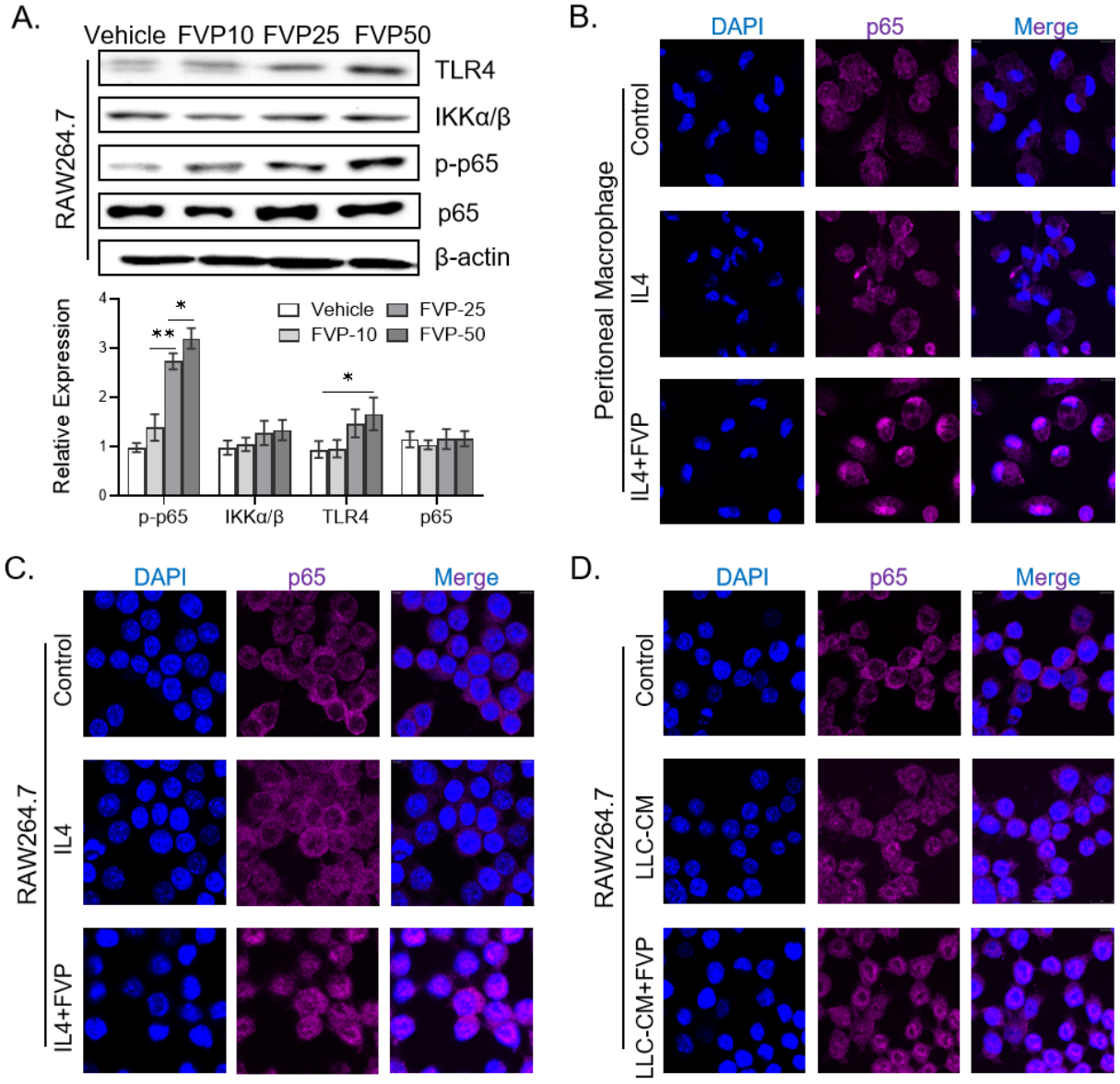

Figure 7 *F. velutipes* polysaccharide induce the activation of TLR4/NF-κB axis
The RAW264.7 and peritoneal macrophages (PMs) were pre-cultured with IL-4 for 2 hours. After the addition of FVP (or PBS) to the medium, the cells were harvested 30 minutes later for immunofluorescence (IF) detection. (A) Immunoblot with anti-phospho-IKKα/β, phospho-p65, p65, TLR4 and β-actin. FVP concentration was 10, 25, 50 μg/mL. (B) Repersentative IF immages of p65 localization in peritoneal macrophages after IL-4 and FVP treatment. (C) Repersentative IF immages of p65 localization in RAW264.7 cells after IL-4 and FVP treatment. (D) IF images of p65 localization in RAW264.7 cells after LLC-CM and FVP treatment. Data represent ≥ 3 independent experiments and are shown as means ± standard deviation. *$P < 0.05$, **$P < 0.01$, ***$P < 0.001$.

This release of the NF-κB complex from its sequestration in the cytoplasm allows it to translocate to the nucleus and regulate the expression of target genes, such as TNF-α, IL-6, and iNOS [9]. Next, we examined the nuclear translocation of NF-κB (p65) in RAW264.7 and peritoneal macrophages via immunofluorescence assay. The results showed that the increased p65 fluorescence intensity was overlaid with the nucleus when

treated with FVP (Figure 7B-D). Furthermore, the LLC-CM also increased p65 fluorescence intensity, and FVP treatment showed a trend for synergy (Figure 7D). Collectively, these results suggest that the activation of the TLR4/NF-κB axis is tightly regulated by FVP to boost anti-tumor immunity (Figure 8).

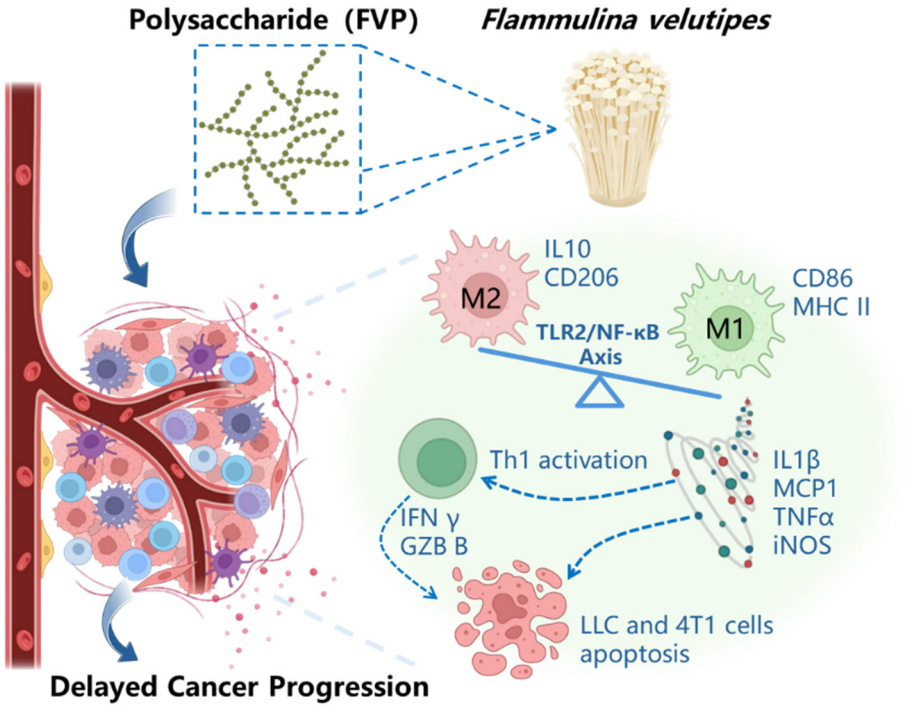

Figure 8 *F. velutipes* polysaccharide boosts the anti-tumor immunity by reversing M1/M2 polarization through TLR4/NF-κB activation

Oral administration of FVP polysaccharide elevated the levels of $CD11b^{+}Ly6C^{high}F4/80^{+}$ macrophages, delayed mammary and lung tumor growth, and increased survival rates in LLC and 4T1 cancer models. Furthermore, FVP reduced the proportion of M2 macrophages and regulatory T cells, which support tumor growth and metastasis, while enhancing pro-inflammatory gene expression, antitumor effects, and Th1 response-related gene expression. These findings suggest that FVP may serve as a promising immunomodulatory agent for reversing macrophage polarization within the tumor microenvironment.

4. Discussion

Cancer immunotherapy activates the immune system to fight cancer cells and can result in complete remission and fewer adverse effects compared to conventional treatments. It can also be combined with other therapies to improve outcomes. Notwithstanding, the immune system is a powerful tool against tumor development, the TME can pose difficulties by suppressing it and inhibiting the activation of immune cells[1, 3]. The cells that possess immune-suppressive functions within the tumor microenvironment include Tregs, myeloid-derived suppressive cells, regulatory dendritic cells, and M2 macrophages[5-7].

In this study, we aimed to elucidate the possible mechanisms underlying the anti-tumor effects of FVP and explore its potential as an agent for reprogramming immune cells. The results show that FVP can significantly delay the progression of LLC and 4T1 carcinoma by regulating M1/M2 macrophage polarization and activating the immune response in both in vitro and in vivo models (Figure 1 and Figure 4). Macrophages are a diverse and versatile group of immune cells that exhibit distinct subpopulations and functions, including the well-known M1 and M2 macrophages[35, 36]. Additionally, tumor-associated macrophages (TAMs), a subtype of M2 macrophages in the tumor microenvironment, have been shown to promote tumor growth and metastasis[8]. Beyond M1 and M2, macrophages also comprise other subpopulations with unique

characteristics. For example, $CD169^+$ macrophages may contribute to the maintenance of immune regulation and tissue homeostasis, while TCR^+ macrophages express CCL2 and possess strong phagocytic capabilities[37]. In conclusion, macrophages are crucial players in immune defense, tissue homeostasis, and disease pathology, with their diverse subpopulations offering promising targets for developing new therapies.

Herein, we found that FVP programmed the IL-4-induced M2 macrophages, and elevate the expression of CD86, CD163, iNOS, and TNF-α (Figure 5). In line with the aforementioned discoveries, FVP was observed to be an inducer for promoting M1-polarization of RAW 264.7 cells [38]. Moreover, in animal experiments, FVP was demonstrated to elevate the expression of IL-1β, iNOS, and ZO-1 genes in the colon tissue of mice [39], while the levels of TNF-α, IFN-γ, IL-6, and IL-8 in mouse serum also increased in a dose-dependent manner [40] (see Figure 6 for reference). From the fruiting bodies of *F. velutipes*, a novel polysaccharide named FVPB2 was isolated and purified. In vitro immunomodulatory studies indicated that FVPB2 can induce the proliferation of mouse spleen lymphocytes in a dose-dependent manner. Furthermore, treatment with FVPB2 increased the levels of IgM and IgG secreted by B cells. Thus, FVPB2 has the potential to be a novel and significant immunomodulatory nutraceutical[41]. Collectively, the aforementioned evidence suggests that FVP possess the capability to reprogram the polarized macrophages, and subfractions such as β-glucan may play a critical role in immune activation [42].

However, a β-type glycosidic polysaccharide isolated from *F. velutipes* has demonstrated efficacy in reducing the levels of TNF-α, IL-6, MCP-1, and MIP-1α in colon tissue and serum, thereby alleviating dextran sodium sulfate-induced ulcerative colitis in mice and achieving remission. In another study, polysaccharides isolated from *F. velutipes* were found to significantly decrease levels of $CD4^+$ and $CD8^+$ T cells, ICAM-1, and MPO in both the serum and colon tissues of normal and burned rats[43]. Additionally, Chen et al. demonstrated that seedbed-like scaffolds derived from FVP accelerate full-thickness skin wound healing and hair follicle regeneration in a green fabrication process [44]. The critical role of M2 macrophages in mediating wound healing has been shown in numerous in vitro and in vivo studies [45]. Besides, *F. velutipes* exhibits better antioxidant activity against hydroxyl radicals and improved metal chelating activity, which suggests that these polysaccharides can be used as natural antioxidants [46, 47]. Oxidative stress can activate a variety of transcription factors, leading to differential expression of genes involved in inflammatory pathways [48]. In summary, the multifaceted functions of FVP are contingent not only upon the specific polysaccharide constituents extracted by researchers, but also upon the distinct pathological milieu in which they operate.

The limitations of this article are evident. In this study, we used a single medium, non-toxic dose of FVP (100 mg/kg/day), previously shown to be immunoregulatory and effective in animal tumour models[10], rather than conducting a formal dose-response analysis. Our primary aim was to elucidate the cellular and molecular mechanisms underlying its anti-tumour activity to inform optimisation of efficacy and future applications. Besides, in the mechanistic study section, we only provided evidence linking FVP treatment to the TLR4/NF-κB pathway, without performing functional validation using pharmacological inhibitors or gene knockdown approaches. In our future endeavors, we aim to carry out the following tasks: categorize the

components of FVP, determine the exact structure of the components that are responsible for reversing M2 macrophage polarization, and screen and identify the receptors of these components.

Comprehensively, this study demonstrated that oral administration of FVP elevated the level of $CD11b^{+}Ly6C^{high}F4/80^{+}$ macrophages, reduced mammary and lung tumor growth, and increased mouse survival rates in LLC and 4T1 cancer models. FVP also decreased the ratio of M2 macrophages and regulatory T cells, which support tumor growth and metastasis, and increased pro-inflammatory gene expression, antitumor effects, and Th1 response gene expression. These findings suggest that FVP has potential as an immunomodulatory agent for modulating macrophage polarization, indicating a potential alternative cancer treatment.

Conflict of Interest

The authors declare no potential conflicts of interest. Yan Zhang is an associate editor for Food Science and Human Wellness and was not involved in the editorial review or the decision to publish this article.

Funding

This work was supported by the National Key Research Project of China (2022YFF1100300), Natural Science Foundation of China (32272328, 81900249), Natural Science Foundation of Hebei Province (B2022321001, H2024206177, H2024206111), National Natural Science Foundation of China (81900249), Hangzhou Normal University University Scientific Research Start-up Fund (4255C50222204096), Shijiazhuang Science and Technology Department (241791417A).

Supplementary Materials

Supplemental Table 1: the primer sequence of RT-PCR analysis

References

1. Zhang, M., C. Liu, J. Tu, et al., *Advances in cancer immunotherapy: historical perspectives, current developments, and future directions.* Mol Cancer, 2025. **24**(1): p. 136 DOI: 10.1186/s12943-025-02305-x.
2. Demols, A., A.M. Bucalau, and L. Mans, *The path to personalized treatment in advanced and metastatic biliary tract cancers: a review of new targeted therapies and immunotherapy.* Curr Opin Oncol, 2022. **34**(4): p. 403–411 DOI: 10.1097/cco.0000000000000850.
3. Pan, Y., C. Yuan, C. Zeng, et al., *Cancer stem cells and niches: challenges in immunotherapy resistance.* Mol Cancer, 2025. **24**(1): p. 52 DOI: 10.1186/s12943-025-02265-2.
4. El-Sayes, N., A. Vito, and K. Mossman, *Tumor Heterogeneity: A Great Barrier in the Age of Cancer Immunotherapy.* Cancers (Basel), 2021. **13**(4) DOI: 10.3390/cancers13040806.
5. Liu, Y., H. Tan, J. Dai, et al., *Targeting macrophages in cancer immunotherapy: Frontiers and challenges.* J Adv Res, 2025. **76**: p. 695–713 DOI: 10.1016/j.jare.2024.12.043.
6. Wang, H., X. Wang, X. Zhang, et al., *The promising role of tumor-associated macrophages in the treatment of cancer.* Drug Resist Updat, 2024. **73**: p. 101041 DOI: 10.1016/j.drup.2023.101041.
7. Toledo, B., L. Zhu Chen, M. Paniagua-Sancho, et al., *Deciphering the performance of macrophages in tumour microenvironment: a call for precision immunotherapy.* J Hematol Oncol, 2024. **17**(1): p. 44 DOI: 10.1186/s13045-024-01559-0.

8. Pan, Y., Y. Yu, X. Wang, et al., *Tumor-Associated Macrophages in Tumor Immunity.* Front Immunol, 2020. **11**: p. 583084 DOI: 10.3389/fimmu.2020.583084.
9. Yin, M., Y. Zhang, and H. Li, *Advances in Research on Immunoregulation of Macrophages by Plant Polysaccharides.* Front Immunol, 2019. **10**: p. 145 DOI: 10.3389/fimmu.2019.00145.
10. Liang, Q., Q. Zhao, X. Hao, et al., *The Effect of Flammulina velutipes Polysaccharide on Immunization Analyzed by Intestinal Flora and Proteomics.* Front Nutr, 2022. **9**: p. 841230 DOI: 10.3389/fnut.2022.841230.
11. Sivanesan, I., M. Muthu, J. Gopal, et al., *Mushroom Polysaccharide-Assisted Anticarcinogenic Mycotherapy: Reviewing Its Clinical Trials.* Molecules, 2022. **27**(13) DOI: 10.3390/molecules27134090.
12. Motta, F., M.E. Gershwin, and C. Selmi, *Mushrooms and immunity.* J Autoimmun, 2021. **117**: p. 102576 DOI: 10.1016/j.jaut.2020.102576.
13. Garcia, J., F. Rodrigues, M.J. Saavedra, et al., *Bioactive polysaccharides from medicinal mushrooms: A review on their isolation, structural characteristics and antitumor activity.* Food Bioscience, 2022. **49**: p. 101955
14. Wong, J.H., T.B. Ng, H.H.L. Chan, et al., *Mushroom extracts and compounds with suppressive action on breast cancer: evidence from studies using cultured cancer cells, tumor-bearing animals, and clinical trials.* Appl Microbiol Biotechnol, 2020. **104**(11): p. 4675–4703 DOI: 10.1007/s00253-020-10476-4.
15. Xu, X., H. Yan, and X. Zhang, *Structure and immuno-stimulating activities of a new heteropolysaccharide from Lentinula edodes.* J Agric Food Chem, 2012. **60**(46): p. 11560–6 DOI: 10.1021/jf304364c.
16. Cheng, H., L. Sun, D. Shen, et al., *Beta-1,6 glucan converts tumor-associated macrophages into an M1-like phenotype.* Carbohydr Polym, 2020. **247**: p. 116715 DOI: 10.1016/j.carbpol.2020.116715.
17. Wang, Y. and H. Zhang, *Advances in the extraction, purification, structural-property relationships and bioactive molecular mechanism of Flammulina velutipes polysaccharides: A review.* Int J Biol Macromol, 2021. **167**: p. 528–538 DOI: 10.1016/j.ijbiomac.2020.11.208.
18. Enokitake, L.T., *Flammulina velutipes: host-mediated antitumor polysaccharides.* Food Rev Intl, 1995. **11**: p. 203–6 DOI: 10.1080/87559129509541033.
19. Xu, H., Y. Hu, Q. Hu, et al., *Isolation, characterization and HepG-2 inhibition of a novel proteoglycan from Flammulina velutipes.* Int J Biol Macromol, 2021. **189**: p. 11–17 DOI: 10.1016/j.ijbiomac.2021.08.086.
20. Chen, G.T., Y.X. Fu, W.J. Yang, et al., *Effects of polysaccharides from the base of Flammulina Velutipes stipe on growth of murine RAW264.7, B16F10 and L929 cells.* Int J Biol Macromol, 2018. **107**(Pt B): p. 2150–2156 DOI: 10.1016/j.ijbiomac.2017.10.090.
21. Zhang, T., J. Ye, C. Xue, et al., *Structural characteristics and bioactive properties of a novel polysaccharide from Flammulina velutipes.* Carbohydr Polym, 2018. **197**: p. 147–156 DOI: 10.1016/j.carbpol.2018.05.069.
22. Euhus, D.M., C. Hudd, M.C. LaRegina, et al., *Tumor measurement in the nude mouse.* J Surg Oncol, 1986. **31**(4): p. 229–34 DOI: 10.1002/jso.2930310402.
23. Niu, Y., J. Dong, H. Jiang, et al., *Effects of Polysaccharide from Malus halliana Koehne Flowers in Cyclophosphamide-Induced Immunosuppression and Oxidative Stress on Mice.* Oxid Med Cell Longev, 2020. **2020**: p. 1603735 DOI: 10.1155/2020/1603735.
24. Fu, C., Z. Fu, C. Jiang, et al., *CD205(+) polymorphonuclear myeloid-derived suppressor cells suppress antitumor immunity by overexpressing GLUT3.* Cancer Sci, 2021. **112**(3): p. 1011–1025 DOI: 10.1111/cas.14783.
25. Cossarizza, A., H.D. Chang, A. Radbruch, et al., *Guidelines for the use of flow cytometry and cell sorting in immunological studies.* Eur J Immunol, 2017. **47**(10): p. 1584–1797 DOI: 10.1002/eji.201646632.
26. Zheng, K., Q. Li, D. Lin, et al., *Peptidomic analysis of pilose antler and its inhibitory effect on triple-negative breast cancer at multiple sites.* Food Funct, 2020. **11**(9): p. 7481–7494 DOI: 10.1039/d0fo01531h.
27. Fu, C., Y. Lu, Y. Zhang, et al., *Intermittent fasting suppressed splenic CD205+ G-MDSC accumulation in a murine breast cancer model by attenuating cell trafficking and inducing apoptosis.* Food Sci Nutr, 2021. **9**(10): p. 5517–5526 DOI: 10.1002/fsn3.2510.
28. Faltusová, K., C.L. Chen, T. Heizer, et al., *Altered Erythro-Myeloid Progenitor Cells Are Highly Expanded in Intensively Regenerating Hematopoiesis.* Front Cell Dev Biol, 2020. **8**: p. 98 DOI: 10.3389/fcell.2020.00098.

29. McAlpine, C.S., M.G. Kiss, S. Rattik, et al., *Sleep modulates haematopoiesis and protects against atherosclerosis.* Nature, 2019. **566**(7744): p. 383–387 DOI: 10.1038/s41586-019-0948-2.
30. Xu, Y., X. Wang, L. Liu, et al., *Role of macrophages in tumor progression and therapy (Review).* Int J Oncol, 2022. **60**(5) DOI: 10.3892/ijo.2022.5347.
31. Wang, S., G. Liu, Y. Li, et al., *Metabolic Reprogramming Induces Macrophage Polarization in the Tumor Microenvironment.* Front Immunol, 2022. **13**: p. 840029 DOI: 10.3389/fimmu.2022.840029.
32. Atri, C., F.Z. Guerfali, and D. Laouini, *Role of Human Macrophage Polarization in Inflammation during Infectious Diseases.* Int J Mol Sci, 2018. **19**(6) DOI: 10.3390/ijms19061801.
33. Kim, H.S., Y.J. Kim, H.K. Lee, et al., *Activation of macrophages by polysaccharide isolated from Paecilomyces cicadae through toll-like receptor 4.* Food Chem Toxicol, 2012. **50**(9): p. 3190–7 DOI: 10.1016/j.fct.2012.05.051.
34. Zhang, L., K. Zhang, J. Zhang, et al., *Loss of fragile site-associated tumor suppressor promotes antitumor immunity via macrophage polarization.* Nat Commun, 2021. **12**(1): p. 4300 DOI: 10.1038/s41467-021-24610-x.
35. Ginhoux, F. and S. Jung, *Monocytes and macrophages: developmental pathways and tissue homeostasis.* Nat Rev Immunol, 2014. **14**(6): p. 392–404 DOI: 10.1038/nri3671.
36. Zhou, J., Z. Tang, S. Gao, et al., *Tumor-Associated Macrophages: Recent Insights and Therapies.* Front Oncol, 2020. **10**: p. 188 DOI: 10.3389/fonc.2020.00188.
37. Chávez-Galán, L., M.L. Olleros, D. Vesin, et al., *Much More than M1 and M2 Macrophages, There are also CD169(+) and TCR(+) Macrophages.* Front Immunol, 2015. **6**: p. 263 DOI: 10.3389/fimmu.2015.00263.
38. Ye, J., X. Wang, K. Wang, et al., *A novel polysaccharide isolated from Flammulina velutipes, characterization, macrophage immunomodulatory activities and its impact on gut microbiota in rats.* J Anim Physiol Anim Nutr (Berl), 2020. **104**(2): p. 735–748 DOI: 10.1111/jpn.13290.
39. Zhao, R., D. Fang, Y. Ji, et al., *In vitro and in vivo functional characterization of an immune activation Flammulina velutipes polysaccharide based on gut microbiota regulation.* Food and Agricultural Immunology, 2020. **31**(1): p. 667–686
40. Zhao, R., Q. Hu, G. Ma, et al., *Effects of Flammulina velutipes polysaccharide on immune response and intestinal microbiota in mice.* Journal of Functional Foods, 2019. **56**: p. 255–264
41. Wang, W.H., J.S. Zhang, T. Feng, et al., *Structural elucidation of a polysaccharide from Flammulina velutipes and its immunomodulation activities on mouse B lymphocytes.* Sci Rep, 2018. **8**(1): p. 3120 DOI: 10.1038/s41598-018-21375-0.
42. Qu, Y., X. Zhao, H. Guo, et al., *Structural analysis and macrophage activation of a novel β-glucan isolated from Cantharellus cibarius.* Int J Mol Med, 2021. **47**(4) DOI: 10.3892/ijmm.2021.4883.
43. Wu, D.M., W.Q. Duan, Y. Liu, et al., *Anti-inflammatory effect of the polysaccharides of golden needle mushroom in burned rats.* Int J Biol Macromol, 2010. **46**(1): p. 100–3 DOI: 10.1016/j.ijbiomac.2009.10.013.
44. Chen, F., Q. Zhang, P. Wu, et al., *Green fabrication of seedbed-like Flammulina velutipes polysaccharides-derived scaffolds accelerating full-thickness skin wound healing accompanied by hair follicle regeneration.* Int J Biol Macromol, 2021. **167**: p. 117–129 DOI: 10.1016/j.ijbiomac.2020.11.154.
45. Kim, S.Y. and M.G. Nair, *Macrophages in wound healing: activation and plasticity.* Immunol Cell Biol, 2019. **97**(3): p. 258–267 DOI: 10.1111/imcb.12236.
46. Zhang, Z., G. Lv, W. He, et al., *Effects of extraction methods on the antioxidant activities of polysaccharides obtained from Flammulina velutipes.* Carbohydr Polym, 2013. **98**(2): p. 1524–31 DOI: 10.1016/j.carbpol.2013.07.052.
47. Yuan, F., Z. Gao, W. Liu, et al., *Characterization, Antioxidant, Anti-Aging and Organ Protective Effects of Sulfated Polysaccharides from Flammulina velutipes.* Molecules, 2019. **24**(19) DOI: 10.3390/molecules24193517.
48. Hussain, T., B. Tan, Y. Yin, et al., *Oxidative Stress and Inflammation: What Polyphenols Can Do for Us?* Oxid Med Cell Longev, 2016. **2016**: p. 7432797 DOI: 10.1155/2016/7432797.